ACADEMIC PRESS

Available online at www.sciencedirect.com

SCIENCE DIRECT®

Journal of Sound and Vibration 269 (2004) 91–111

JOURNAL OF SOUND AND VIBRATION

www.elsevier.com/locate/jsvi

Parameter identification of vehicles moving on continuous bridges

F.T.K. Au*, R.J. Jiang, Y.K. Cheung

Department of Civil Engineering, The University of Hong Kong, Pokfulam Road, Hong Kong, People's Republic of China

Received 5 June 2002; accepted 19 December 2002

Abstract

This paper describes a method for the identification of parameters of vehicles moving on multi-span continuous bridges. Each moving vehicle is modelled as a 2-degree-of-freedom system that comprises four components: an unsprung mass and a sprung mass, which are connected together by a damper and a spring. The corresponding parameters of these four components, namely, the equivalent unsprung mass and sprung mass, the damping coefficient and the spring stiffness are identified based on dynamic simulation of the vehicle–bridge system. The identification process makes use of acceleration measurements at selected stations on the bridge. In the study, the acceleration measurements are simulated from the solution to the forward problem of a continuous beam under moving vehicles, together with the addition of artificially generated measurement noise. The identification is carried out through a robust multi-stage optimization scheme based on genetic algorithms, which searches for the best estimates of parameters by minimizing the errors between the measured accelerations and the reconstructed accelerations from the moving vehicles. This multi-stage optimization scheme reduces the variable search domains stage by stage using the identified results of the previous stage. Besides the basic operators in simple genetic algorithms, some advanced genetic operators and techniques are adopted here. Therefore, it makes the proposed identification procedure much more efficient than other traditional optimization methods. The identification procedure is then verified with a few test cases. The estimated vehicle parameters can also be used to get the time varying contact forces between the vehicles and bridge surface.

1. Introduction

Parameter identification is an important kind of problem relevant to many fields, and various researchers have experimented with different optimization methods and techniques. For the

*Corresponding author. Tel.: +1-2859-2650; fax: +1-2559-5337.
E-mail address: francis.au@hku.hk (F.T.K. Au).

0022-460X/03/$ - see front matter
doi:10.1016/S0022-460X(03)00005-1

identification of vehicle parameters, one of the traditional tools is the least squares method [1–3] and its amended versions [2]. The other methods for identification of vehicle parameters include the extended Kalman filter method [4,5], the maximum likelihood method [6], and the recursive prediction error method [7]. A comparative study [8] has been carried out on the last three methods of identification of vehicle parameters, and the study has discovered that the most common problem with these optimization methods is convergence. Different models have been created to represent the actual behaviour of vehicles with different emphasis. For models of vehicle–tyre system with different numbers of degrees-of-freedom (d.o.f.s) [1,3,6,8], different numbers of system parameters are identified. In some cases, attention is paid to the driver–vehicle interaction analysis [9] and the vehicle parameters for riding quality optimization [4,10]. At other times, the aim of parameter identification is to get the tyre forces and the road friction coefficients for vehicles on different road surfaces [11]. Most of the identifications mentioned above are realized based on the simulated or experimental test data of the vehicles.

From the point of view of dynamic coupling between the vehicle and the road, the motion of a bridge is largely related to the motion of a vehicle on it. This is well verified by the results of forward analysis of bridge dynamics under moving loads [12] and moving vehicles [13]. All the forward dynamic analysis of bridges under moving vehicles is based on the assumption that the vehicle parameter values are known correctly. However, for the normal operation and structural health monitoring of existing bridges open to public, it is unrealistic to expect that all the correct vehicle parameters are known beforehand. Therefore the identification of vehicle parameters is an important step in the study of dynamic behaviour of existing bridges.

This paper describes a method for the identification of parameters of vehicles moving on multi-span continuous bridges. Instead of just modelling the vehicles as moving masses [14], each moving vehicle is modelled as a 2-d.o.f. system [13] that comprises four components: an unsprung mass and a sprung mass, which are connected together by a damper and a spring. The corresponding parameters of these four components, namely, the equivalent unsprung mass and sprung mass, the damping coefficient and the spring stiffness are identified based on the acceleration measurements at various stations along the continuous beam. In the study, the acceleration measurements are simulated from the solution to the forward problem of a continuous beam under moving vehicles based on the modified vibration functions [12] and modal superposition, together with the addition of artificially generated measurement noise.

The identification is carried out through a robust multi-stage optimization scheme based on genetic algorithms [15], which searches for the best estimates of parameters by minimizing the errors between the measured accelerations and the reconstructed accelerations from the moving vehicles. This multi-stage optimization scheme reduces the variable search domains stage by stage using the identified results of the previous stage. Based on the mechanics of natural selection and natural genetics, genetic algorithms combine survival of the fittest among string structures with a structured yet randomized information exchange to form a search algorithm with some of the innovative flair of human search. Their special search mechanics leads to their special robust function of finding the global optimal values of the variables definitely without worrying about the convergence problem nor the restrictive requirements of continuity and derivative existence, as compared with the traditional optimization techniques. Apart from the basic strategies of simple genetic algorithms, other advanced genetic techniques, such as niching, elitism, fitness scaling, are also adopted to improve the efficiency. In the present parameter identification problem, a natural

search domain that contains all the possible options for each variable does not exist, at least at the initial stage of solution. In order to overcome this problem and to improve the efficiency, a multi-stage optimization procedure based on genetic searching is put forward by reducing the variable search domains stage by stage using the identified results of the previous stage.

A comprehensive case study is then carried out to verify the robustness of the proposed identification method. The effects of different noise levels, various parameters used in the genetic algorithms, the number of measurement stations, and the number of vehicles on the results are studied. The time-dependent contact forces between the moving vehicles and the bridge surface can also be calculated from the identified vehicle parameters. The work described in this paper will be useful to the operation and structural health monitoring of existing bridges.

2. Simulation of acceleration measurements

2.1. Modelling of vehicles and bridge

In this paper, a multi-span continuous bridge is modelled as a linear elastic Bernoulli–Euler beam with totally $(P+1)$ point supports as shown in Fig. 1. The bridge may have varying sections characterized by the density $\rho(x)$, cross-sectional area $A(x)$, Young's modulus $E(x)$ and moment of inertia $I(x)$ at location x. The N moving vehicles on the bridge are modelled as 2-d.o.f. systems each with four parameters $\{M_{s1}, M_{s2}, c_s, k_s, s=1,2, \ldots, N\}$. The typical sth moving vehicle is modelled by the unsprung mass M_{s1} and the sprung mass M_{s2}, which are interconnected by a spring of stiffness k_s and a dashpot of damping coefficient c_s. The convoy of vehicles moves from left to right along the bridge at a speed $v(t)$. Setting the position of the leftmost point support of the bridge as the origin O, the horizontal position of the sth vehicle is defined as $x_s(t)$, a function of t. The deflection of the bridge at position x and at time t is denoted by $y(x,t)$ where upward deflection is taken as positive, as shown in Fig. 1. The vertical displacements of the unsprung mass and sprung mass of sth vehicle are, respectively, represented by $\{y_{s1}(t), y_{s2}(t), s=1,2\ldots,N\}$, which are also measured vertically upwards with reference to their respective vertical positions before coming onto the bridge.

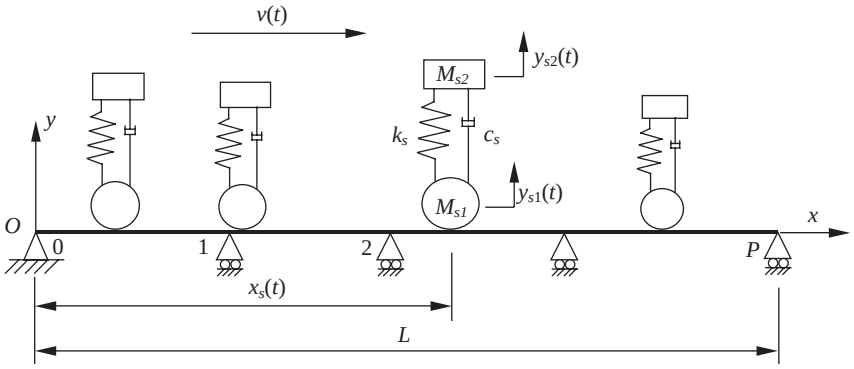

Fig. 1. A multi-span continuous bridge with N moving vehicles.

If the surface roughness of the bridge and the separation of the vehicle from the bridge are neglected, the vertical displacement $y_{s1}(t)$ of the unsprung mass of the sth vehicle model is the same as the deflection of the beam $y(x_s(t), t)$ at the corresponding location $x_s(t)$. Then the vertical displacement $y_{s1}(t)$ and its first two derivatives are as follows:

$$y_{s1}(t) = y(x, t)|_{x=x_s(t)}, \tag{1}$$

$$\frac{\mathrm{d}y_{s1}(t)}{\mathrm{d}t} = \left[\frac{\partial y(x,t)}{\partial t} + \frac{\partial y(x,t)}{\partial x}v\right]\Bigg|_{x=x_s(t)}, \tag{2}$$

$$\frac{\mathrm{d}^2 y_{s1}(t)}{\mathrm{d}t^2} = \left[\frac{\partial^2 y(x,t)}{\partial t^2} + 2v\,\frac{\partial^2 y(x,t)}{\partial x \cdot \partial t} + v^2\,\frac{\partial^2 y(x,t)}{\partial x^2} + a\,\frac{\partial y(x,t)}{\partial x}\right]\Bigg|_{x=x_s(t)}, \tag{3}$$

where a is the horizontal acceleration of the group of vehicles. The contact force $f_{cs}(t)$ between the sth unsprung mass and the beam can be expressed as

$$f_{cs}(t) = (M_{s1} + M_{s2})g + \Delta f_{cs}(t), \tag{4}$$

in which g is the acceleration due to gravity and $\Delta f_{cs}(t)$ is the time-dependent variation of contact force.

The equation of vertical motion for the sth unsprung mass M_{s1} and sprung mass M_{s2} can be written as

$$M_{s1}\frac{\mathrm{d}^2 y_{s1}(t)}{\mathrm{d}t^2} = \Delta f_{cs}(t) + k_s[y_{s2}(t) - y_{s1}(t)] + c_s\left[\frac{\mathrm{d}y_{s2}(t)}{\mathrm{d}t} - \frac{\mathrm{d}y_{s1}(t)}{\mathrm{d}t}\right], \tag{5}$$

$$M_{s2}\frac{\mathrm{d}^2 y_{s2}(t)}{\mathrm{d}t^2} = -k_s[y_{s2}(t) - y_{s1}(t)] - c_s\left[\frac{\mathrm{d}y_{s2}(t)}{\mathrm{d}t} - \frac{\mathrm{d}y_{s1}(t)}{\mathrm{d}t}\right]. \tag{6}$$

From Eqs. (4)–(6), the contact force between the sth vehicle and the bridge can be written as

$$f_{cs}(t) = (M_{s1} + M_{s2})g + \left(M_{s1}\frac{\mathrm{d}^2 y_{s1}(t)}{\mathrm{d}t^2} + M_{s2}\frac{\mathrm{d}^2 y_{s2}(t)}{\mathrm{d}t^2}\right). \tag{7}$$

For the modelling of the continuous bridge, the modified vibration functions [12] are chosen, which are built up from the vibration modes of a hypothetical single-span simply supported beam having the same end supports and total length as the real beam, and cubic spline expressions that ensure the boundary conditions at the supports. Therefore the assumed vibration modes can be written as

$$\Phi_i(x) = \bar{\Phi}_i(x) + \tilde{\Phi}_i(x), \tag{8}$$

where $\{\bar{\Phi}_i(x), i = 1, 2, \ldots, n\}$ are the first n vibration modes of a hypothetical beam of total length L with the same end supports but without the intermediate supports, and $\{\tilde{\Phi}_i(x), i = 1, 2, \ldots, n\}$ are the augmenting cubic spline expressions which are so chosen that each $\Phi_i(x)$ satisfies the boundary conditions at the two ends and the zero deflection conditions at the intermediate point supports. For a hypothetical beam that is simply supported, the vibration modes $\bar{\Phi}_i(x)$ are the Fourier sine series. The augmenting cubic spline expressions $\tilde{\Phi}_i(x)$ can be determined by using the zero deflection conditions at the intermediate supports and the boundary conditions at end supports.

By modal superposition and separation of variables, the vibration of the beam can be expressed as

$$y(x,t)=\sum_{i=1}^{n} q_i(t)\Phi_i(x) \quad (i=1,2,\ldots,n), \tag{9}$$

where $q_i(t)$ are the generalized coordinates.

2.2. Simulation of noise-free acceleration measurements

Based on the vehicle and bridge models introduced above, dynamic analysis of the system can be carried out and the simulated noise-free acceleration measurements at specified stations of the bridge can be obtained for the subsequent parameter identification of the vehicles. This part is in fact a conventional forward problem. The velocity of vibration and the curvature of the beam at position x are, respectively,

$$\frac{\partial y(x,t)}{\partial t}=\sum_{i=1}^{n} \dot{q}_i(t)\ \Phi_i(x), \tag{10}$$

$$\frac{\partial^2 y(x,t)}{\partial x^2}=\sum_{i=1}^{n} q_i(t)\Phi_i''(x), \tag{11}$$

in which the dot represents differentiation with respect to time t, and the prime represents differentiation with respect to the abscissa x. Therefore the kinetic energy T, the bending energy V, and the work done by external forces W are, respectively,

$$T=\frac{1}{2}\int_0^L \rho(x)A(x)\left[\frac{\partial y(x,t)}{\partial t}\right]^2 \mathrm{d}x=\frac{1}{2}\sum_{i=1}^{n}\sum_{j=1}^{n}\dot{q}_i(t)m_{ij}\dot{q}_j(t), \tag{12}$$

$$V=\frac{1}{2}\int_0^L E(x)I(x)\left[\frac{\partial^2 y(x,t)}{\partial x^2}\right]^2 \mathrm{d}x=\frac{1}{2}\sum_{i=1}^{n}\sum_{j=1}^{n}q_i(t)k_{ij}q_j(t), \tag{13}$$

$$W=-\int_0^L \sum_{s=1}^{N} f_{cs}y(x,t)\delta[x-x_s(t)]\,\mathrm{d}x=\sum_{i=1}^{n} q_i(t)f_i(t), \tag{14}$$

where the work done by external forces W is defined in terms of the Dirac delta function

$$\delta(x-x_0)=\begin{cases}\infty & (x=x_0)\\ 0 & (x\neq x_0)\end{cases} \tag{15a}$$

$$\int_{-\infty}^{\infty}\delta(x-x_0)\,\mathrm{d}x=1, \tag{15b}$$

while m_{ij}, k_{ij} and $f_i(t)$ are, respectively, the generalized mass, stiffness and force, which can be written as

$$m_{ij} = \int_0^L \rho(x)A(x)\Phi_i(x)\Phi_j(x)\,\mathrm{d}x, \tag{16}$$

$$k_{ij} = \int_0^L E(x)I(x)\Phi_i''(x)\Phi_j''(x)\,\mathrm{d}x, \tag{17}$$

$$f_i(t) = \sum_{s=1}^{N}(-f_{cs}\Phi_i[x_s(t)]) = \sum_{s=1}^{N} f_{is}(t). \tag{18}$$

The component $f_{is}(t)$ in the generalized force $f_i(t)$ can be further written as

$$\begin{aligned} f_{is}(t) = & -(M_{s1}+M_{s2})g\Phi_i(x_s(t)) - M_{s2}\ddot{y}_{s2}(t)\Phi_i(x_s(t)) \\ & - M_{s1}\Phi_i(x_s(t))\sum_{j=1}^{n}\{\ddot{q}_j(t)\Phi_j(x_s(t)) + 2v\dot{q}_j(t)\Phi_j'(x_s(t)) + q_j(t)[v^2\Phi_j''(x_s(t)) + a\Phi_j'(x_s(t))]\}. \end{aligned} \tag{19}$$

The Lagrangian function for the vehicle-bridge system is $\Gamma = T - (V - W)$, where $(V - W)$ is the total potential energy, and the Euler-Lagrange equation appears as

$$\frac{\mathrm{d}}{\mathrm{d}t}\left(\frac{\partial\Gamma}{\partial\dot{q}_i}\right) - \frac{\partial\Gamma}{\partial q_i} = 0. \tag{20}$$

Substituting Eqs. (16–17) and (18) into Eq. (20) gives

$$\sum_{j=1}^{n}\hat{m}_{ij}\ddot{q}_j(t) + \sum_{j=1}^{n}\hat{c}_{ij}\dot{q}_j(t) + \sum_{j=1}^{n}\hat{k}_{ij}q_j(t) = \hat{p}_i(t), \quad i = 1, 2, \ldots, n, \tag{21}$$

where

$$\hat{m}_{ij}(t) = m_{ij} + \sum_{s=1}^{N} M_{s1}\Phi_i(x_s(t))\Phi_j(x_s(t)), \tag{22}$$

$$\hat{c}_{ij}(t) = \sum_{s=1}^{N} 2vM_{s1}\Phi_i(x_s(t))\Phi_j'(x_s(t)), \tag{23}$$

$$\hat{k}_{ij}(t) = k_{ij} + \sum_{s=1}^{N} M_{s1}\Phi_i(x_s(t))\left[v^2\Phi_j''(x_s(t)) + a\Phi_j'(x_s(t))\right], \tag{24}$$

$$\hat{p}_i(t) = -\sum_{s=1}^{N}(M_{s1}+M_{s2})g\Phi_i(x_s(t)). \tag{25}$$

Should a particular vehicle be outside the bridge, the corresponding terms under the summation signs should be omitted.

Eq. (21) can be solved by the Newmark-β method. Therefore $\{q_i(t)\}$ and $\{\ddot{q}_i(t)\}$ can be obtained accordingly. The simulated "noise-free" acceleration $a_{nf}(x,t)$ of the beam at measurement

location x can then be expressed as

$$a_{nf}(x,t) = \ddot{y}(x,t) = \sum_{i=1}^{n} \ddot{q}_i(t)\Phi_i(x). \tag{26}$$

The vector containing the simulated "noise-free" acceleration time histories at the measurement stations then forms the noise-free acceleration vector $\boldsymbol{A}_{nf}$.

2.3. Simulation of measurement noise

In practical experiments or fieldwork, the measurements are usually polluted by measurement noise. To evaluate the sensitivity of the results to such measurement noise, noise-polluted measurements are simulated by adding to the noise-free acceleration vector a corresponding noise vector whose root-mean-square (RMS) value is equal to a certain percentage of the r.m.s. value of the noise-free data vector. The components of all the noise vectors are of Gaussian distribution, uncorrelated and with a zero mean and unit standard deviation. Then the noise-polluted acceleration $\mathbf{A}_{np}$ of the bridge at location x can be simulated by

$$\mathbf{A}_{np} = \mathbf{A}_{nf} + \mathrm{RMS}\,(\mathbf{A}_{nf}) \cdot N_{level} \cdot \mathbf{N}_{\mathrm{unit}}, \tag{27}$$

where $\mathrm{RMS}(\mathbf{A}_{nf})$ is the root-mean-square value of the noise-free acceleration vector $\mathbf{A}_{nf}$, N_{level} is the noise level, and $\mathbf{N}_{unit}$ is the randomly generated noise vector with zero mean and unit standard deviation. In the present study, besides the case of zero noise, five levels of noise pollution will be investigated, namely 5, 10, 15, 20% and 25%.

3. Multi-stage parameter identification based on genetic algorithms

3.1. Genetic algorithms

Genetic algorithms [15] are stochastic global search techniques based on the mechanics of natural selection and natural genetics. They combine survival of the fittest among string structures with a structured yet randomized information exchange to form a search algorithm with some of the innovative flair of human search. The central theme of genetic algorithms is robustness, which results from their special search ways, namely, working with a coding of the parameter set, not the parameters themselves; searching from a population of points, not a single point; using objective function information, not derivatives or other auxiliary knowledge; and using probabilistic transition rules, not deterministic rules. Because of these intrinsic characteristics, the search and optimization direction of genetic algorithms is definitely guided to global optimal values of the variables instead of the local optimal solution in traditional search and optimization methods. Convergence is not a problem for genetic algorithms at all. Genetic algorithms have found applications in a wide spectrum of areas, covering problems with discrete variables and continuous variables.

In the present study, the variables to be identified are the equivalent unsprung mass and sprung mass, the damping coefficient and the spring stiffness for each vehicle. Assuming that there are all together N vehicles on a bridge, the number of parameters to be identified is therefore $4N$. All the

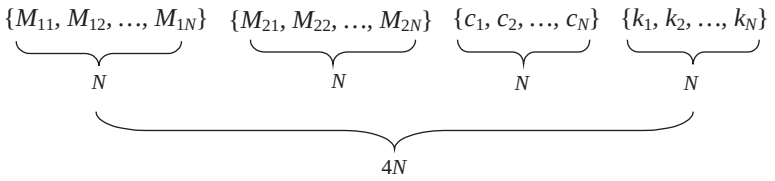

Fig. 2. The structure of an individual with $4N$ variables in the present study.

parameters are coded as binary strings with different string lengths, where the string length is defined as the number of the binary bits for one variable. For the purpose of optimization using genetic algorithms, these strings are assembled together in prescribed order to form individuals, and the structure of an individual adopted in the present study is shown in Fig. 2. To kick off the search and optimization process, a specified number of individuals must be randomly created to form an initial population.

3.2. Genetic techniques adopted

The three basic genetic operations in simple genetic algorithms are adopted here, namely reproduction of individuals, crossover between individuals in a population, and the mutation of individuals. Besides these, a few advanced genetic techniques are used, which improves the identification efficiency in each stage. After an initial population is randomly created with the specified population size, the tournament selection scheme is used with a shuffling technique for choosing random pairs for mating. In order to keep the fittest individuals in the later populations, elitism is also included, which means that the best individuals in a generation will be reproduced to the next generation. Uniform crossover is adopted for the proposed identification process. Jump mutation or creep mutation scheme is used to realize mutation. Niche theory is also introduced. A sharing function used to induce niche in this genetic algorithm limits the uncontrolled growth of particular species within a population.

Another important improvement scheme—linear fitness scaling [15] is implemented to keep appropriate levels of competition throughout a simulation. Without scaling of the objective function values, there is a tendency for a few super-individuals to dominate the selection process early on during a run, which is a leading cause of premature convergence. In this case, the objective function values must be scaled down to prevent a takeover of the population by these super-strings. Later on during the run, when the population is largely converged, competition among population members is less strong and the simulation tends to wander. In this case, the objective function values must be scaled up to accentuate differences between population members to continue to reward the best performers. In both cases, at the beginning of the run and as the run matures, the linear fitness scaling can help.

The fitness value is related to the objective function to reflect the desirability of the individual. Linear scaling requires a linear relationship between the scaled fitness f' and the raw fitness f as follows:

$$f' = af + b. \tag{28}$$

The coefficients a and b are chosen based on two criteria. The first is to enforce equality of the average value f_{avg} of the raw fitness values and the average value f'_{avg} of the scaled fitness values. The second criterion is to control the number of offspring given to the population member with maximum raw fitness. In particular, the best population member is expected to give C_{mult} copies in the next generation, i.e.,

$$f'_{\max} = C_{mult} f_{avg}, \tag{29}$$

where $f'_{\max}$ is the maximum scaled fitness. Here C_{mult} is taken as 2.0, which means that the number of expected copies desired for the best population member is 2.

In the present identification of vehicle parameters, the errors at the measurement stations between the measured or simulated accelerations and the reconstructed accelerations from the identified vehicle parameters should be minimized. For a bridge with Q measurement stations and a total of R time points in each measured time history, the objective function F to be maximized in the present study can be written in terms of the error vector $\mathbf{e}_i$ as

$$F = -\sum_{i=1}^{Q} \|\mathbf{e}_i\|_2 = -\sum_{i=1}^{Q} \left(\sum_{j=1}^{R} (e_{ij})^2 \right)^{1/2}, \tag{30}$$

where $\|\mathbf{e}_i\|_2$ is the Euclidean vector norm of the error vector $\mathbf{e}_i$ defined as

$$\mathbf{e}_i = \{a_{ij,simu}\} - \{a_{ij,iden}\}, \tag{31}$$

where $a_{ij,simu}$ is the element of the simulated acceleration vector and $a_{ij,iden}$ is the element of the acceleration vector calculated from the trial identified vehicle parameters in each generation, both at the ith measurement station and the jth time point.

Linear scaling works well except when negative fitness calculation prevents its use [15]. To overcome this problem associated with Eq. (30), a mapping from the objective function F to the raw fitness f is carried out as

$$f = F + C_{\min}, \tag{32}$$

where C_{min} is chosen to enforce that the raw fitness f is always positive. In the present study, the value of C_{min} is taken to be the absolute value of the worst objective function value in each current generation, which prevents the occurrence of the negative fitness in every generation.

3.3. Multi-stage optimization

In the present parameter identification problem, a natural search domain that contains all the possible options for each variable does not exist obviously, at least at the initial stage of solution. Although the identification of the contact forces provides useful clues to the identification of moving masses [14], this may not be as useful here. In order not to miss the global optimal set of parameters and converge on a wrong solution, the initial search domain for each variable must be set sufficiently large. However within these very large search domains, it is often difficult to find the ideal global optimal values by a single optimization run, and it also takes an extremely long running time. Without any idea of the likely magnitudes of the optimal parameters, it is difficult to determine the appropriate string lengths, which are essential for accurate results. In order to overcome this problem, the parameter identification is carried out through a multi-stage

optimization scheme involving the repeated use of genetic algorithms and gradual refinement of search domains as well as accuracy. Using reasonable string lengths and a relatively small number of generations, it is possible for the initial stage of optimization to produce rough estimates of the parameters. Such estimates are then used to map out the refined search domains for the second stage. It is known that the genetic optimization gradually guides the trial solutions to the optimal one. Therefore through this staged optimization process, the search domains will be reducing in each successive stage in the light of the identification results of the previous stage until the desired identification precision is reached.

In the present study, all parameters to be identified are non-negative values, and so the lower limits of their initial search domains are all set as zero. The upper limits of the initial search domains for the spring stiffness and the damping coefficient are set to 10^{20} or even larger values in standard units. For both the unsprung and sprung masses for normal bridges, a convenient upper limit of the initial search domain can be taken as 10^6 kg. These search domains can then be narrowed down in subsequent stages of optimization. For example, assuming the identified unsprung mass of the sth vehicle in a stage to be $M_{s1,iden}$, the search domain D of this unsprung mass for the next stage can be set as

$$D = (D_l, D_u) = M_{s1,iden}(C_l, C_u), \quad 0 < C_l < 1 \quad 1 < C_u, \tag{33}$$

where C_l and C_u are, respectively, coefficients to define the lower limit D_l and the upper limit D_u of the search domain D. The same strategy can be applied to the search for parameters for the sprung mass M_{s2}, the spring stiffness k_s and the damping coefficient c_s. The values of C_l and C_u may be varied at different stages for improved efficiency. The termination of the search at each stage is controlled both by the changes of parameters between successive generations as well as the maximum number of generations allowed. However the termination of the whole optimization procedure is controlled by the differences between the identified parameters of consecutive stages. The efficiency of this multi-stage optimization process based on genetic algorithms at each stage will be verified by a comprehensive case study.

4. Case study

4.1. General description

To evaluate the efficiency and effectiveness of the proposed method, a comprehensive case study covering various aspects have been carried out. The effects of population sizes, number of measurement stations, levels of measurement noise, and number of vehicles on the accuracy are examined. Table 1 summarizes the different aspects examined in various cases. The contact forces between the moving vehicles and the bridge surface are also estimated using the identified vehicle parameters. The identification error $Error_{iden}$ of, for example, the unsprung mass of sth vehicle is defined as

$$Error_{iden} = \frac{|M_{s1,iden} - M_{s1,true}|}{M_{s1,true}} \times 100\%, \tag{34}$$

Table 1
Cases for investigation

Case	No. of vehicles	No. of stations	Noise level (%)	Population size	Effects to investigate
1	1	1	0	30	Basic strategy
2	1	1	5	5, 10, 20, 30, 40, 60, 80, 100	Population size
3	1	1	5, 10, 15, 20, 25	30	Measurement noise
4	1	1, 2, 3, 4, 6	10	30	Number of stations
5	3	2, 6	10	60	Number of vehicles

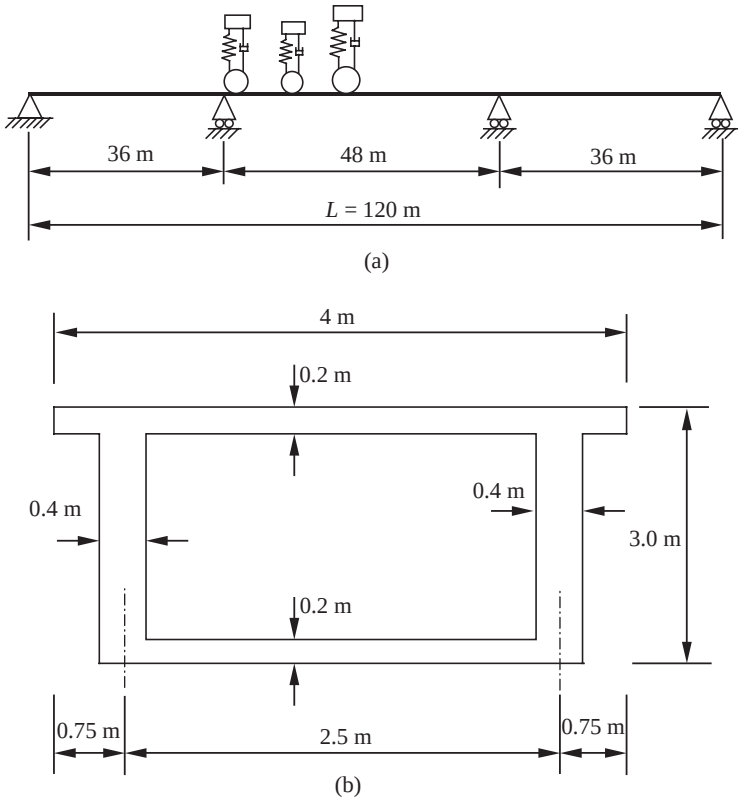

Fig. 3. A three-span continuous bridge. (a) Idealized beam model; (b) idealized cross-section.

where $M_{s1,iden}$ and $M_{s1,true}$ are the identified and true values of unsprung mass M_{s1}, respectively. A similar definition is also applied to other parameters such as the sprung mass, spring stiffness and damping coefficient.

A three-span continuous box girder bridge is used in the case study, and the idealized beam model and cross-section are shown in Fig. 3. The density ρ and Young's modulus E of concrete are 2400 kg/m^3 and 30 000 Mpa, respectively. The span lengths from left to right are 36, 48, 36 m, respectively. The cross-sectional area A and the second moment of inertia I are 3.46 and 3.854 m^4, respectively. For both the acceleration simulation and parameter identification, the first three

vibration modes of the bridge are adopted. All the vehicles are assumed to travel at a horizontal speed v of 17 m/s across the bridge. Both for the simulation of acceleration measurements and the subsequent analysis, the total traversing time T, which is counted from the instant when the first vehicle arrives at the starting end of the bridge to that when the last vehicle leaves the bridge, is divided into 200 time intervals. The histories of acceleration and contact forces are therefore presented accordingly with respect to time ratio t/T. The contact forces between the vehicles and the bridge surface are calculated from

$$f_{cs}(t) = -(M_{s1}+M_{s2})g\Phi_i(x_s(t)) - M_{s2}\ddot{y}_{s2}(t)\Phi_i(x_s(t)) - M_{s1}\Phi_i(x_s(t))\sum_{j=1}^{n}\{\ddot{q}_j(t)\Phi_j(x_s(t)) + 2v\dot{q}_j(t)\Phi_j'(x_s(t)) + q_j(t)[v^2\Phi_j''(x_s(t)) + a\Phi_j'(x_s(t))]\}. \quad (35)$$

The parameters for the present genetic algorithm with uniform crossover are as follows: crossover probability $P_c = 0.5$, creep mutation probability $P_{cm} = 0.04$, and jump mutation probability $P_{jm} = 1/N_{pop}$, where N_{pop} denotes the population size. As seen in the following cases, where the signals are not contaminated with measurement noise, essentially the true parameters are obtained.

4.2. Case study 1: basic strategy

In Case 1, there is only one moving vehicle with simulated noise-free accelerations at the measurement station located at the middle of the central span, i.e., $x = 60$ m. This is mainly to establish the validity and effectiveness of this multi-stage optimization procedure. The true parameters for the vehicle used are the unsprung mass $M_1 = 4800$ kg, the sprung mass $M_2 = 27000$ kg, the damping coefficient $c = 86000$ Ns/m, and the spring stiffness $k = 9.12 \times 10^6$ N/m. These parameters are applicable to the other cases unless otherwise stated.

In the first optimization stage, the initial search domains of the four vehicle parameters are set as $M_1 \in (0, 10\,000)$ kg, $M_2 \in (0, 60\,000)$ kg, $c \in (0, 200\,000)$ Ns/m and $k \in (0, 2 \times 10^7)$ N/m, and their string lengths are 7, 8, 8 and 8, respectively. The population size is set as 30. By generation 300 of the first stage, the identified parameters M_1, M_2, c and k are 4961, 26 824 kg, 89 412 Ns/m and 9.098×10^6 N/m, respectively. Based on these identified values, and taking the coefficients C_l and C_u for Eq. (33) as 0.9 and 1.1, respectively, the search domains are narrowed down to $M_1 \in (4465, 5457)$ kg, $M_2 \in (24\,142, 29\,506)$ kg, $c \in (80\,471, 98\,353)$ Ns/m and $k \in (8.188 \times 10^6, 10.0078 \times 10^6)$ N/m. Similarly, the genetic search is carried out again within these refined search domains. The identified parameters in this stage are then used to map out the search domains for the next stage. In this manner, the correct results are gradually identified as shown in Table 2. Only three stages are necessary to get the essentially true values of the parameters. The redefinition of search domains for successive stages enables the identification process to be both accurate and efficient.

Table 3 shows the evolution of results for the first stage. The maximum number of generations for this stage is set as 800. It can be seen that among the first 90 generations, the results change a lot, while the results in generations 244–800 are essentially the same. Therefore the chosen number of generations is enough for the first stage, and it can be safely terminated.

Table 2
Case 1: summary of results at different stages noise-free measurements, station at x=60 m, population size = 30

Stage	Limit coefficients for search domain		Identified parameters			
	C_l	C_u	M_1 (kg)	M_2 (kg)	c (Ns/m)	k(N/m)
1	—	—	4961	26 824	89 412	9 098 039
2	0.9	1.1	4729	27 292	88 167	9 224 698
3	0.95	1.05	4802	27 002	86 038	9 120 620
True value			4800	27 000	86 000	9 120 000
Error (%)			0.04	0.01	0.04	0.01

Table 3
Case 1: evolution of results in the first stage (noise-free measurements, station at x=60 m, population size = 30)

Generation number	Identified parameters			
	M_1 (kg)	M_2 (kg)	c (Ns/m)	k (N/m)
1–5	7874	25647	71373	9 254 902
6–7	2992	29412	144314	9 725 490
8	6457	25647	69804	9 333 333
9–11	2835	29882	96470	9 725 490
12	4094	29412	94902	9 882 353
13–17	4094	29412	96471	9 725 490
18	3780	29412	97255	9 725 490
19–24	3780	29412	99608	9 725 490
25–26	4409	29176	99608	9 725 490
27–28	3937	28941	99608	9 647 059
29	4724	28470	99608	9 568 627
30–31	3937	28470	99608	9 568 627
32–33	3780	28470	99608	9 411 765
34–39	3937	28470	99608	9 490 196
40	4252	28470	99608	9 490 196
41–54	4094	28471	99608	9 490 196
55	4094	28471	98039	9 490 196
56–69	4330	28235	98039	9 490 196
70–73	4252	28235	98039	9 411 765
74–88	4252	28235	94902	9 411 765
89–243	4252	28235	96471	9 411 765
244–800	4961	26824	89412	9 098 039
Error (%)	3.35	0.65	3.97	0.24

4.3. Case study 2: effect of population size

This is essentially the same as Case 1 except that 5% measurement noise is introduced and that the population size is varied to study its effect on the accuracy and efficiency of the method.

Table 4
Case 2: effects of population size on accuracy. (5% measurement noise, station at x=60 m)

Population size	Number of stages	Identified values				Errors (%)			
		M_1 (kg)	M_2 (kg)	c (Ns/m)	k (N/m)	M_1	M_2	c	k
5	4	4778	27052	86 728	9 118 394	0.46	0.19	0.85	0.02
10	3	4758	27035	86 147	9 095 260	0.88	0.13	0.17	0.27
20	3	4790	26942	85 267	9 106 979	0.21	0.22	0.85	0.14
30	2	4775	27042	85 668	9 107 513	0.52	0.15	0.39	0.14
40	2	4774	27035	85 806	9 118 959	0.55	0.13	0.23	0.01
60	2	4775	26957	86 229	9 109 327	0.52	0.15	0.27	0.12
80	2	4792	26963	85 845	9 141 072	0.17	0.14	0.18	0.23
100	2	4780	26963	86 192	9 113 324	0.42	0.14	0.22	0.07

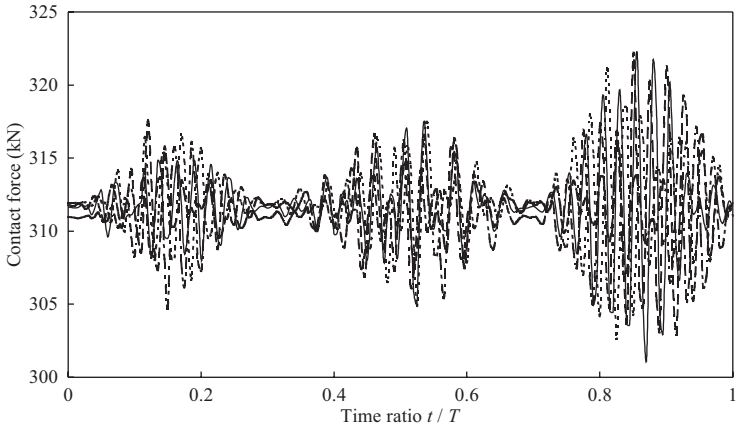

Fig. 4. Case 2: contact forces calculated from the true and identified vehicle parameters using different population sizes: —— true; – – – size = 5; — — size = 30; — – — size = 60.

Starting from the initial search domains $M_1 \in (0,\ 10\,000)$ kg, $M_2 \in (0,\ 60\,000)$ kg, $c \in (0,\ 200\,000)$ Ns/m and $k \in (0.2 \times 10^7)$ N/m, the proposed identification method is applied with eight different kinds of population sizes, namely 5, 10, 20, 30, 40, 60, 80 and 100. The results are summarized in Table 4. First and foremost, no matter what population size is used, extremely good results are obtained with errors less than 1%. For population sizes larger than 20, results of comparable accuracy are obtained after the second stage. The computation time required for the larger population sizes of 40, 60, 80 and 100 is of course much longer than that for a smaller population size. However for a population size of 5, at least four stages are needed to get results comparable to those obtained from two stages with population sizes larger than 20. In other words, a population size that is too small reduces the speed by requiring more optimization stages, while a population size that is too large increases the computation time in each optimization stage. A population size of 30 is considered appropriate to the parameter identification of a single moving vehicle.

Table 5
Case 3: effects of measurement noise on accuracy (station at x=60 m, population size = 30)

Noise level (%)	Number of stages	Identified values				Errors (%)			
		M_1 (kg)	M_2 (kg)	c (Ns/m)	k (N/m)	M_1	M_2	c	k
5	2	4775	27 042	85 668	9 107 513	0.52	0.15	0.39	0.14
10	3	4812	27 136	86 474	9 113 098	0.25	0.50	0.55	0.08
15	3	4774	26 962	85 855	9 162 722	0.54	0.14	0.17	0.47
20	3	4783	26 783	85 491	9 127 093	0.35	0.80	0.59	0.08
25	3	4762	27 185	86 006	9 147 911	0.79	0.69	0.01	0.31

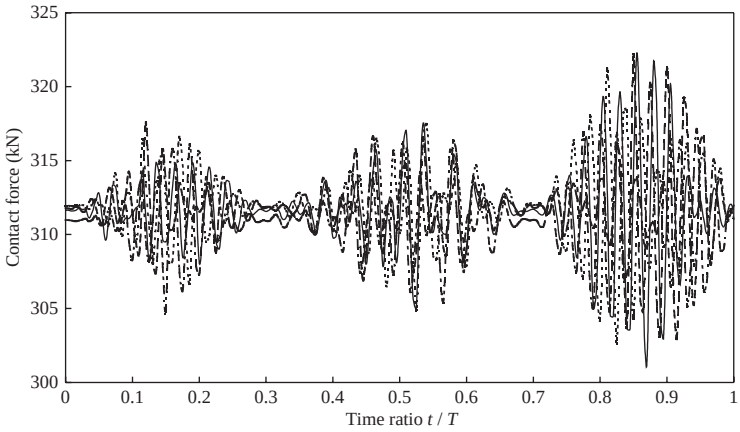

Fig. 5. Case 3: contact forces calculated from the true and identified vehicle parameters using measurements of different noise levels: —— true; – – – 5% noise; — — 10% noise.

The histories of contact forces calculated from the identified parameters using different population sizes are plotted in Fig. 4 and compared with the true values. Very good agreement is observed.

4.4. Case study 3: effect of measurement noise

The effect of measurement noise on the accuracy and efficiency of the proposed method is next investigated. This case is essentially the same as Case 1 except that five measurement noise levels of 5%, 10%, 15%, 20% and 25% are introduced. Following the conclusions of the studies for Case 2, a population size of 30 is adopted for this identification problem with a single moving vehicle. Table 5 shows the identification results, from which it can be seen that the identification values vary little with the increase of the measurement noise level. This demonstrates that the proposed identification procedure is not particularly sensitive to measurement noise levels. For the five noise levels, the errors are still well below 1%. However the more measurement noise there is, the more optimization stages are required. Fig. 5 shows the identified contact forces based on noise-free measurements, and measurements with noise levels of 5% and 10%. Basically, very

Table 6
Case 4: arrangement of measurement stations

Numbers of measuring stations	Locations of measuring stations, x (m)
1	60
2	18, 60
3	18, 60, 102
4	18, 52, 68, 102
6	12, 24, 52, 68, 96, 108

Table 7
Case 4: effects of number of measurement stations

Number of measurement stations	Number of stages	Identified values				Errors (%)			
		M_1 (kg)	M_2 (kg)	c (Ns/m)	k (N/m)	M_1	M_2	c	k
5% *measurement noise, population size* = 30									
1	2	4775	27 042	85 668	9 107 513	0.52	0.15	0.39	0.14
2	2	4813	27 019	86 424	9 110 873	0.27	0.07	0.49	0.10
3	2	4808	26 982	86 149	9 106 786	0.17	0.07	0.17	0.15
4	2	4814	26 875	85 887	9 087 109	0.30	0.09	0.07	0.36
6	2	4781	26 967	85 777	9 116 734	0.40	0.12	0.26	0.04
10% *measurement noise, population size* = 30									
1	3	4812	27 136	86 474	9 113 098	0.25	0.50	0.55	0.08
2	3	4793	27 038	86 464	9 110 588	0.15	0.14	0.54	0.10
3	3	4827	26 882	85 798	9 097 493	0.56	0.44	0.23	0.25
4	2	4773	27 012	85 767	9 099 936	0.56	0.04	0.27	0.22
6	2	4799	26 962	85 777	9 115 070	0.02	0.14	0.26	0.05
20% *measurement noise, population size* = 30									
1	3	4783	26 783	85 491	9 127 093	0.35	0.80	0.59	0.08
2	3	4844	26 948	86 114	9 088 694	0.92	0.19	0.13	0.34
3	3	4821	27 024	85 743	9 106 786	0.44	0.09	0.30	0.15
4	2	4819	27 106	85 862	9 123 056	0.39	0.39	0.16	0.03
6	2	4814	27 011	85 777	9 092 955	0.30	0.04	0.26	0.30

good agreement is observed although the presence of noise in the measurements does give rise to certain discrepancies.

4.5. Case study 4: effect of number of measurement stations

Very often more than one accelerometer is used in field measurements. It not only improves the accuracy in most cases, but also caters for the possibility of occasional breakdown of certain instruments. The case of an increased number of measurement stations is studied. For comparison, the identification problem is repeated using five patterns of measurement stations, namely, 1, 2, 3, 4 and 6 measurement stations, respectively. The distribution and locations of the

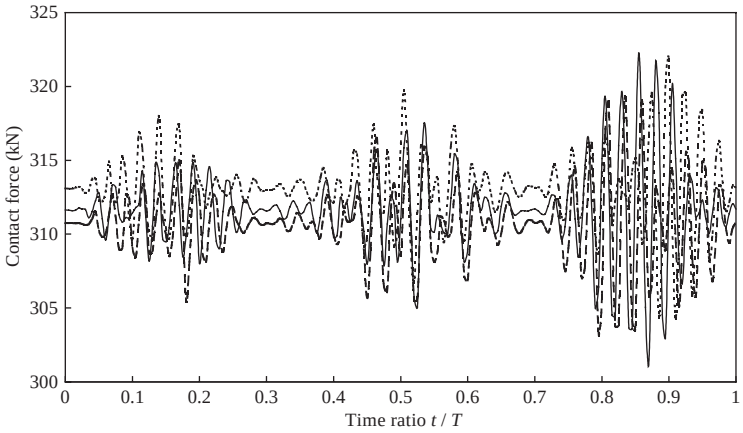

Fig. 6. Case 4: contact forces calculated from the true and identified vehicle parameters using different number of measurement stations: —— true; – – – One station; — — three stations.

Table 8
Case 5: assume true vehicle parameters

Vehicle	Unsprung mass (kg)	Sprung mass (kg)	Damping coefficient (Ns/m)	Spring stiffness (N/m)
1	4800	27 000	86 000	9.12×10^6
2	3900	24 000	72 000	8.68×10^6
3	5400	32 000	100 000	10.0×10^6

measurement stations for each arrangement are summarized in Table 6. A population size of 30 is used and three levels of measurement noise, namely 5%, 10% and 20%, are considered. The identification results as shown in Table 7 are very good. The errors are well below 1% even for 20% measurement noise. Similar to what is seen before, the higher the measurement noise, the more stages are needed. With the same level of measurement noise, the efficiency of optimization in general increases with the number of measurement stations, as seen in the number of stages required. However this is achieved at the expense of computation time.

The time histories of the contact forces calculated from the true and identified values of the vehicle parameters using 1 and 3 measurement stations with 10% measurement noise are plotted in Fig. 6. It is obvious that the time histories of contact forces calculated from identified parameters both agree well with the true time histories, but that identified based on three measurement stations is closer to the true one.

4.6. Case study 5: effect of number of vehicles

In real life, there are always many vehicles on a bridge at the same time. In order to test the accuracy and efficiency of the proposed method for more practical situations, a convoy comprising three vehicles at a spacing of 10 m is considered and their true parameters are shown in Table 8. Both the two and six-station measurement arrangements are used, and their locations are shown in Table 6. The measurement noise for acceleration simulation is taken to be 10%. The

Table 9
Case 5: effect of number of vehicles (10% measurement noise, population size = 60)

Parameters		Identified values		Errors (%)		Number of stages
		Two stations	six stations	Two stations	Six stations	
Vehicle 1	M_{11} (kg)	4757	4807	0.90	0.15	
	M_{12} (kg)	27266	27065	0.99	0.24	
	c_1 (Ns/m)	85790	86196	0.24	0.23	
	k_1 (N/m)	9237977	9131049	1.29	0.12	
Vehicle 2	M_{21} (kg)	3861	3881	1.00	0.49	
	M_{22} (kg)	23988	23979	0.00	0.09	4
	c_2 (Ns/m)	73212	71482	1.68	0.72	
	k_2 (N/m)	8711342	8709654	0.36	0.34	
Vehicles 3	M_{31} (kg)	5465	5429	1.20	0.54	
	M_{32} (kg)	32276	31901	0.86	0.31	
	c_3 (Ns/m)	101615	100165	1.62	0.17	
	k_3 (N/m)	10068262	10062176	0.68	0.62	

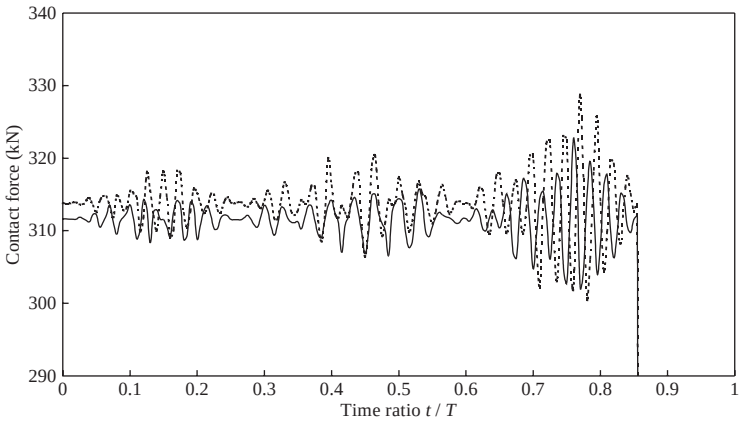

Fig. 7. Case 5: contact forces of the first vehicle calculated from the true and identified vehicle parameters using two measuring stations: —— true; – – – identified.

same initial search domains as in Case 1 are used. In view of the larger number of parameters to be identified in this case, the population size is set as 60. The identification results as shown in Table 9 are very good. For example, in the two-station measurement arrangement, identification errors below 2% can be obtained after only four optimization stages even though there are 12 parameters to be identified. In the six-station measurement arrangement, identification error below 1% can be obtained after only four optimization stages. It demonstrates that the proposed method can also cope with a convoy of vehicles with reasonable accuracy although longer computation time is required for more vehicles. It is also seen that the accuracy improves when more measurement stations are used. For the present three-span continuous bridge, six measurement stations are sufficient for parameter identification of the vehicle convoy.

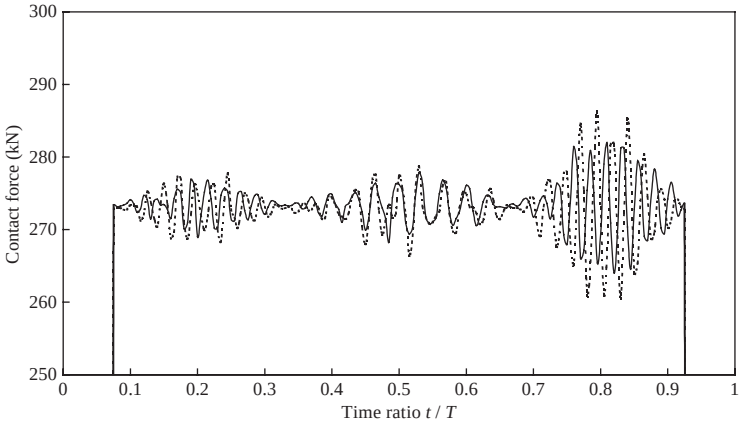

Fig. 8. Case 5: contact forces of the second vehicle calculated from the true and identified vehicle parameters using two measuring stations: —— true; – – – identified.

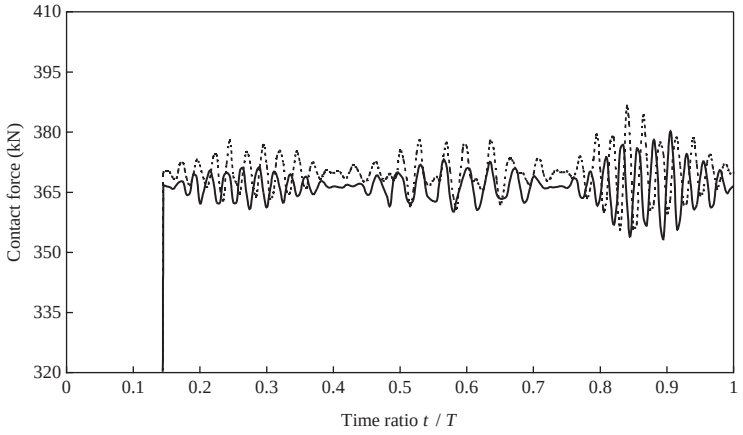

Fig. 9. Case 5: contact forces of the third vehicle calculated from the true and identified vehicle parameters using two measuring stations: —— true; – – – identified.

The time histories of contact forces of the three vehicles calculated from the true and identified parameters using two measurement stations are plotted in Figs. 7–9, respectively. Note that the total traversing time T is counted from the instant when the first vehicle arrives at the starting end of the bridge to that when the last vehicle leaves the bridge. Therefore the time history for each vehicle only occupies part of the total traversing time. Good agreement is again observed.

5. Discussions

In Case 1 when noise-free simulated accelerations are used, effectively the exact results are obtained. It shows that the proposed procedure is theoretically correct and accurate. Then in the other cases, the procedure is tested on various aspects including the population size, noise level of

acceleration measurements, number of measurement stations, and number of vehicles. Examination of the results confirms that the identification method is very robust. Even for a larger number of variables and a reasonably high noise level, very acceptable results can be obtained after only a few optimization stages with an appropriate population size. In all the five cases studied above, even only a few measurement stations are chosen along the whole bridge, very acceptable results can be obtained no matter how many vehicles are on the bridge at the same time.

6. Conclusions

A procedure for the identification of vehicles moving on multi-span continuous bridges is described. The moving vehicles are modelled as 2-d.o.f. systems each comprising an unsprung mass and a sprung mass interconnected by a damper and a spring. The aim of the study is to identify the associated vehicle parameters based on the acceleration measurements at selected stations. Here the acceleration measurements are simulated by the numerical solution to the associated forward problem with random noise introduced to account for the likely errors in practice. The search for the vehicle parameters is formulated as an optimization problem in which the error between the measured accelerations and the accelerations reconstructed from trial vehicle parameters is minimized. A robust multi-stage optimization scheme based on genetic algorithms has been proposed in which the search domains are systematically reduced to converge on the optimal solution. A comprehensive study has been carried out to test the proposed procedure. It shows that in spite of the presence of measurement noise, accurate results are still obtained. The method can also cope with the presence of multiple vehicles and the use of instruments at multiple sections.

Acknowledgements

The work described in this paper has been supported by the Committee on Research and Conference Grants, The University of Hong Kong, China. The present study has made use of the code of a genetic algorithm written by Dr. D.L. Carroll at the University of Illinois, and this is gratefully acknowledged.

References

[1] C.A. Julien, H.M. Hung, Technique in system identification for dynamic mechanical systems, SAE-Paper 690497, 1969, p. 9.

[2] R. Schlegemilch, M. Railey, System identification comparison study, Proceedings of the 21st Annual Pittsburgh Conference Part 5 (of 5), Pittsburgh, PA, May 3–4, 1990, pp. 2269–2273.

[3] Y. Kyongsu, K. Hedrick, Observer-based identification of nonlinear system parameters, Journal of Dynamic Systems, Measurement and Control, Transactions of the American Society of Mechanical Engineers 117 (2) (1995) 175–182.

[4] K. Wise, R.E. Reid, Modeling and identification of a light truck engine mounting system for ride quality optimization, International Congress & Exposition—Society of Automotive Engineers, Warrendale, PA, 1984, 841142P.
[5] D.A. Derradji, N. Mort, Multivariable adaptive control using artificial neural networks, Proceedings of the 1996 UKACC International Conference on Control. Part 2 (of 2), Exeter, UK, September 2–5 1996, 427/2, pp. 889–893.
[6] P. Michelberger, J. Bokor, A. Keresztes, P. Varlaki, Identification of a multivariable linear model for road vehicle dynamics from test data, International Journal of Vehicle Design 8 (1) (1987) 96–114.
[7] K.R. Goheen, E.R. Jefferys, The application of alternative modelling techniques to ROV dynamics. Proceedings of the 1990 IEEE International Conference on Robotics and Automation, Cincinnati, OH, May 13–18 1990, pp. 1302–1309.
[8] D.H. Lee, J.G. Lee, Comparison of parameter identification algorithms for flight vehicles, Transactions of the Japan Society for Aeronautical and Space Sciences 36 (114) (1994) 249–256.
[9] E. Bisimis, Use of system identification methods for the determination of vehicle parameters from measured time histories, Vehicle System Dynamics 6 (1977) 182–184.
[10] O. Kropac, J. Sprinc, Identification of the system vehicle-road parameters, Vehicle System Dynamics 11 (4) (1982) 241–249.
[11] L.R. Ray, Nonlinear tire force estimation and road friction identification: simulation and experiments, Automatica 33 (10) (1997) 1819–1833.
[12] D.Y. Zheng, Y.K. Cheung, F.T.K. Au, Y.S. Cheng, Vibration of multi-span non-uniform beams under moving loads by using modified beam vibration functions, Journal of Sound and Vibration 212 (3) (1998) 455–467.
[13] Y.K. Cheung, F.T.K. Au, D.Y. Zheng, Y.S. Cheng, Vibration of multi-span non-uniform bridges under moving vehicles and trains by using modified beam vibration functions, Journal of Sound and Vibration 228 (3) (1999) 611–628.
[14] R.J. Jiang, F.T.K. Au, Y.K. Cheung, Identification of masses moving on multi-span beams based on genetic algorithms, Computers and Structures 81 (22–23) (2003) 2137–2148.
[15] D.E. Goldberg, Genetic Algorithms in Search Optimization, and Machine Learning, Addison-Wesley Reading, MA, 1989.